Heliyon 10 (2024) e27314

Contents lists available at ScienceDirect

Heliyon

journal homepage: www.cell.com/heliyon

Research article

Quantitative assessment of brown adipose tissue whitening in a high-fat-diet murine model using synthetic magnetic resonance imaging

Mengjuan Huo [a,b,1], Junzhao Ye [c,1], Yinhong Zhang [a,1], Meng Wang [a], Jialu Zhang [d], Shi-Ting Feng [a], Huasong Cai [a,**], Bihui Zhong [c,***], Zhi Dong [a,*]

[a] *Department of Radiology, The First Affiliated Hospital, Sun Yat-sen University, 58th, The Second Zhongshan Road, Guangzhou 510080, China*
[b] *Department of Radiology, The Second Affiliated Hospital of Guangzhou University of Chinese Medicine, 111 Dade Road, Yuexiu District, Guangzhou 510120, China*
[c] *Department of Gastroenterology, The First Affiliated Hospital, Sun Yat-sen University, 58th, The Second Zhongshan Road, Guangzhou 510080, China*
[d] *MRI Research, GE Healthcare, Beijing 10076, China*

ARTICLE INFO

Keywords:
Brown adipose tissue
Whitening
Synthetic magnetic resonance imaging
Transverse relaxation time
Longitudinal relaxation time

ABSTRACT

Purpose: This study aimed to quantitatively evaluate the whitening process of brown adipose tissue (BAT) in mice using synthetic magnetic resonance imaging (SyMRI) and analyzed the correlation between SyMRI quantitative measurements of BAT and serum lipid profiles.
Methods: Fifteen C57BL/6 mice were divided into three groups and fed different diets as follows: normal chow diet for 12 weeks, NCD group; high-fat diet (HFD) for 12 weeks, HFD-12w group; and HFD for 36 weeks, HFD-36w group. Mice were scanned using 3.0 T SyMRI. T1 and T2 values of BAT and interscapular BAT (iBAT) volume were measured. After sacrifice, the body weight of mice, lipid profiles, BAT morphology, and uncoupling protein 1 (UCP1) levels were determined. Statistical analysis was performed using one-way analysis of variance or Kruskal–Wallis test followed by Bonferroni correction for pairwise comparisons. Bonferroni-adjusted significance level was set at $P < 0.017$ (alpha: $0.05/3 = 0.017$).
Results: T2 values of BAT in the HFD-12w group were significantly higher than those in the NCD group ($P < 0.001$), and those in the HFD-36w group were significantly higher than those in the other two groups (both $P < 0.001$). The iBAT volume in the HFD-36w group was significantly higher than that in the HFD-12w ($P = 0.013$) and NCD groups ($P = 0.005$). T2 values of BAT and iBAT volume were significantly correlated with serum lipid profiles and mouse body weight.
Conclusions: SyMRI can noninvasively evaluate the whitening process of BAT using T2 values and iBAT volume, thereby facilitating the visualization of the whitening process.

* Corresponding author. Department of Radiology, The First Affiliated Hospital, Sun Yat-Sen University, 58th, The Second Zhongshan Road, Guangzhou, Guangdong, China.
** Corresponding author. Department of Radiology, The First Affiliated Hospital, Sun Yat-Sen University, 58th, The Second Zhongshan Road, Guangzhou, Guangdong, China.
*** Corresponding author. Department of Gastroenterology, The First Affiliated Hospital, Sun Yat-sen University, 58th, The Second Zhongshan Road, Guangzhou, Guangdong, China.
E-mail addresses: caihuas@mail.sysu.edu.cn (H. Cai), zhongbh@mail.sysu.edu.cn (B. Zhong), dongzh7@mail.sysu.edu.cn (Z. Dong).
[1] These authors contributed equally to this work.

https://doi.org/10.1016/j.heliyon.2024.e27314
Received 6 May 2023; Received in revised form 17 February 2024; Accepted 27 February 2024
Available online 9 March 2024

1. Introduction

Obesity and its related disorders have been the top health challenges in the modern population, leading to increasing experimental research on the functional mechanism of two major adipose tissues in mammals: white adipose tissue (WAT) and brown adipose tissue (BAT). WATs are composed of white adipocytes and mainly store energy in the form of triglycerides in large lipid droplets. In contrast, BATs are composed of brown adipocytes with numerous mitochondria and consume energy via uncoupling protein 1 (UCP1) by utilizing free fatty acids to promote non-shivering thermogenesis [1,2]. High-fat diet (HFD) is a well-known obesity-inducing factor; obese mice can gradually transform BAT into WAT through a process called BAT whitening. Different characteristic changes, such as large lipid droplet accumulation, mitochondrial dysfunction or loss, decreased UCP1 expression and vascular endothelial growth factor (VEGF), as well as tissue inflammation [3–5], can be induced by BAT whitening, resulting in excess ectopic fat accumulation, which is a major risk factor for developing hyperlipidemia, type 2 diabetes, and cardiovascular diseases [6]. Moreover, BAT whitening may store more triglycerides and reduce energy expenditure to induce or even aggravate obesity and associated metabolic disorders [1,2]. Therefore, BAT whitening is a potential therapeutic target for preventing and treating obesity and related metabolic diseases.

An increasing number of studies have directed drug development to increase energy expenditure to suppress BAT whitening [7,8]. Assessment of drug efficacy is required to measure the degree of changes in BAT whitening, which is mainly dependent on histopathology [5,9]. However, detecting typical human brown adipocytes is challenging because of BAT whitening, in which most adipocytes in the body are gradually replaced by unilocular adipocytes with a white-like appearance [1,2]. Furthermore, a repeated biopsy is an invasive procedure that is not accepted by most patients, rendering brown adipocytes undetectable. Therefore, a noninvasive method is urgently required for the quantitative assessment of BAT whitening. Recently, the BAT of mice has been revealed to be similar to that of humans under certain physiological conditions, suggesting that mice are a good model for translational studies of BAT [9–11]. To the best of our knowledge, no study has quantitatively assessed BAT whitening using noninvasive imaging methods yet.

Synthetic magnetic resonance imaging (SyMRI) is a novel technique that allows for obtain quantitative values for tissue-specific properties, such as longitudinal relaxation time (T1), and transverse relaxation time (T2) within a single scan by simultaneously generating T1-and T2-weighted images [12,13]. SyMRI can distinguish BAT from WAT via the differences between the relaxation times of two adipose tissues, and interscapular BAT (iBAT) volume can be measured noninvasively through synthetic T2-weighted images (*s*T2WI) [14]. The relaxation times of the tissues can reflect their various compositions. For adipose tissues, a pilot study has demonstrated a disparity in T1 relaxation time between individuals with severe obesity and normal weight [15]. In general, BAT whitening caused by chronic obesity could alter the cytoarchitecture of BAT, manifested as enlarged lipid droplets, cholesterol crystallization, collagen fiber wrapping, and mitochondrial loss [1,7], which results in ultrastructural changes in BAT and affects its relaxation time. Moreover, BAT plays an important role in regulating lipid metabolism, which can be disrupted by long-term HFD and whitened BAT, leading to an increase in the serum levels of triglycerides (TG), total cholesterol (TC), and low-density lipoprotein cholesterol (LDL-C) [16,17]. To the best of our knowledge, the correlation between SyMRI quantitative measurements of BAT and serum lipid profiles, such as serum levels of TG, TC, LDL-C, and high-density lipoprotein cholesterol (HDL-C), has not yet been reported.

Therefore, we aimed to investigate the whitening process of BAT with SyMRI and determine whether quantitative measurements of BAT from SyMRI could reflect alterations in the serum lipid profiles.

2. Materials and methods

2.1. Animal care and group design

Fifteen C57BL/6J mice, aged 8–10 weeks, were obtained from the Nanjing Biomedical Research Institute of Nanjing University (Nanjing, China). All animals were maintained in an environment with a relative humidity of 50–60%, temperature of 22 ± 2 °C, and a light/dark cycle (12-h light, 12-h dark) with free access to water and food before MRI scanning. All mice were acclimatized with a normal chow diet and water for the first week and then randomly divided into three groups according to the following feed instructions: (1) the NCD group (n = 5) was fed a normal chow diet (10% kcal from fat, 20% kcal from protein, 70% kcal from carbohydrates) for 12 weeks; (2) the HFD-12w group (n = 5) was fed HFD (Dyets D-112252: 60% kcal from fat, 20% from protein, 20% kcal from carbohydrates) for 12 weeks; and (3) the HFD-36w group (n = 5) was fed HFD for 36 weeks.

2.2. Measurement of body weight

Body weight was measured before the dietary intervention to ensure the lack of significant difference in the average body weight among the three groups. The body weight of each mouse was measured thrice at the end of the experiment (before dissection) and recorded as the average value.

2.3. SyMRI scanning and postprocessing

After the mice were anesthetized using pentobarbital sodium at a dose of 40 mg/kg body weight via intraperitoneal (i.p.) injection, all MR examinations were performed using a 3.0 T scanner (SIGNA Pioneer, GE Healthcare, Milwaukee, WI) equipped with a 5-cm diameter animal-suitable receive coil in the prone position, centered around the interscapular region of the mouse.

For SyMRI, the axial and sagittal sections were obtained using a two-dimensional multi-saturation delay, multi-echo fast spin-echo

(MDME) sequence which contains two echo times and four automatically calculated saturation delays (inversion times, TI). As a result, the raw data from the MDME sequence for each slice were composed of eight complex images [18,19]. The detailed parameters of the MDME sequence were presented below: repetition time range, 4400 to 4517 ms; echo time, 24.3 and 121.4 ms; field of view, $9 \times 9\ cm^2$; image matrix, 352×352; bandwidth, 27.78 kHz; slice thickness, 2 mm; slice spacing, 0 mm; slice number, 20; and echo train length, 16.

An offline post-processing software (synthetic MRI 8.0; Synthetic MR, Linköping, Sweden) was used to simultaneously generate synthetic T1-weighted images (sT1WI), sT2WI and quantitative maps (T1 and T2 maps) from the MDME raw data.

The T1 and T2 values of BAT and subcutaneous WAT (sWAT) were measured by a region-of-interest (ROI)-based method [19,20]. On axial sT2WI, the ROIs for iBAT were manually outlined along the edge of the iBAT slice-by-slice, avoiding the blood vessels as much as possible. And ROIs for the dorsal sWAT were also manually delineated on the slices showing iBAT ROIs. Finally, the T1 and T2 values of BAT and sWAT were obtained by calculating the mean quantitative values of all pixels within the ROIs. The iBAT volume was obtained by merging all the ROIs of the iBAT on contiguous slices of the axial sT2WI. The ROI outlines for iBAT and sWAT were independently performed by a radiologist with 10 years of MRI experience, and the accuracy of the ROIs was checked by another radiologist with 15 years of MRI experience and familiarity with mouse anatomy.

2.4. Measurement of serum lipid profiles

After MR scanning, the mice were anesthetized, and blood samples were collected by enucleation of mouse eyeballs after mice were fasted overnight for 12 h. The serum was separated from the whole blood and preserved for further biochemical testing. TG, TC, LDL-C, and HDL-C serum levels were analyzed using commercial assay kits (Jian Cheng Bioengineering Institute, Nanjing, China).

2.5. Dissection of iBAT and sWAT and histological analysis

After blood sample collection, a surgical incision was made in the interscapular region to excise the BAT depots and dorsal sWAT. The iBAT and sWAT samples were fixed in 10% formalin for 24 h, embedded in paraffin, serially sectioned to 4 μm, and stained with hematoxylin and eosin (HE) according to standard procedures.

For axial anatomical reference, cryosection was performed using a separate adult mouse that did not belong to the imaging cohort. The cadaver was peeled from base of skull to bottom of thoracic cavity, and separately severed at the horizontal cross-sections of the upper and lower borders of the scapula. Subsequently, the specimen was embedded in OCT and frozen for 25 min at -25° for preparation of cryosections. Finally, the specimen was sectioned layer by layer using a cryo-section machine, and photographed.

2.6. UCP1 quantification

BAT sections were dewaxed and rehydrated before antigen retrieval, which involved heating the tissue sections in a microwave with EDTA buffer (pH 9). The sections were incubated with 3% hydrogen peroxide for 25 min to block endogenous peroxidase, rinsed with phosphate-buffered saline (PBS), incubated with 3% bovine serum albumin (BSA), followed by rabbit anti-UCP1 (1:500, ab 10983; Abcam, Cambridge, UK) primary antibody incubation overnight. Finally, the secondary antibody incubation was performed for 50 min with horseradish peroxidase-conjugated goat anti-rabbit immunoglobulin G (1:200, GB23303; Servicebio, Wuhan, China).

Three microscopic fields showing the highest immunopositivity for each positive section were selected for UCP1 quantitative analysis, and photomicrographs were captured at a magnification ($40 \times$). UCP1 quantitative analysis was assessed using the means of the immunopositive area fraction of UCP1 using ImageJ software (version 1.8.0). In the photomicrographs, the immunopositive area fraction was automatically measured as the positive immunoreaction, which was defined by the immunopositive area as a percentage of the total area of the microscopic field [21,22]. The mean immunopositive area fraction for each case was calculated.

2.7. Statistical analysis

Our study aimed to verify whether statistically significant differences existed among the three groups in T1 and T2 values of BAT and sWAT, iBAT volume, body weight, lipid profiles, and UCP1. The results are expressed as mean $\pm$ SD and tested for normality and homogeneity of variances before statistical analysis. With satisfactory parametric test conditions, the differences among the three groups were analyzed using one-way analysis of variance (ANOVA) followed by Bonferroni correction for multiple comparisons. Otherwise, differences were analyzed using the Kruskal–Wallis test followed by Bonferroni correction for pairwise comparisons. The Bonferroni-adjusted significance level was set at $P < 0.017$ (alpha: $0.05/3 = 0.017$).

Pearson or Spearman analyses were performed to determine the correlation between quantitative variables. A P value < 0.05 was considered statistically significant. Correlations with a coefficient >0.8 were considered strong, those with values from 0.8 to 0.5 were considered moderate, those with values from 0.5 to 0.3 were considered weak, and those with values below 0.3 were considered nearly nonexistent [23]. All statistical analyses were performed using SPSS Statistics (version 25.0; IBM Corp., Armonk, NY, USA).

3. Results

3.1. BAT morphology and UCP1 quantitative analysis

Visual inspection after anatomical dissection revealed that the colour of iBAT were brown in NCD group (Fig. 1A and B), Sulzer's vein was clear visible (Fig. 1B), after feeding on HFD for 12 weeks, the colour of iBAT seems unchanged (Fig. 1C and D), however, after feeding on HFD for 36 weeks, iBAT became white in appearance (Fig. 1E and F), indicating loss of BAT content. This visual change was confirmed by HE staining of BAT. Fig. 2 shows the histological results of HE-stained BAT in the three groups, visually illustrating how the HDF-induced progress of whitening altered the architecture of BAT. The NCD group showed a multilocular pattern of lipid storage in a typical BAT form (Fig. 2A). The HFD-12w group exhibited a small number of large unilocular adipocytes accumulated in the brown adipocytes compared with that in the NCD group, showing slight BAT whitening (Fig. 2B). Notably, compared with the other two groups, the chronic intake of HFD in the HFD-36w group yielded progressive damage in the BAT multilocular cytoarchitecture, resulting in a pronounced increase in large unilocular adipocyte accumulation. Moreover, the brown adipocytes of the HFD-36w group had a complete disarrangement in structure and resembled the lipid storage pattern of white adipocytes, indicating more severe BAT whitening (Fig. 2C). Adipocytes within the sWAT initially appeared to be unilocular but became larger during the whitening process (Fig. 2D–F).

Fig. 3 shows immunohistochemical (IHC) staining for UCP1 expression and the quantitative UCP1 expression results of BAT in the three groups. IHC staining for UCP1 revealed positive immunoreactions in all groups (Fig. 3A–C); however, the UCP1-positive area decreased in the HFD-36w group owing to numerous white-like adipocytes in BATs (Fig. 3C). No statistically significant differences were detected between the NCD and HFD-36w groups in the immunopositive area fraction of UCP1 ($P > 0.017$). However, the immunopositive area fraction of UCP1 showed significantly decreased UCP1 expression in the HFD-36w group compared with that in the NCD and HFD-12w groups ($P < 0.001$, $P = 0.001$, respectively) (Fig. 3D).

3.2. Alterations in T1 and T2 values of BAT and sWAT, and iBAT volume during BAT whitening

Fig. 4 shows the representative SyMRI images of iBAT in the three groups and photograph of axial cryosection. The Kruskal–Wallis test revealed no significant difference in the distribution of the T1 values of BAT and sWAT among the three groups ($P = 0.852$, $P = 0.171$, respectively) (Fig. 5A and B), whereas one-way ANOVA revealed a statistically significant difference in the average T2 values of BAT among the three groups ($F = 73.557$, $P < 0.0001$). Further analysis with the Bonferroni test indicated that the mean T2 values in the HFD-12w group (71.91 ± 4.07 ms) were significantly higher than those in the NCD group (66.14 ± 4.98 ms, $P < 0.001$), and those in the HFD-36w group (83.07 ± 5.70 ms) were significantly higher than those in the other two groups (both $P < 0.001$) (Fig. 5C).

The Kruskal–Wallis test revealed a statistically significant difference in the distribution of T2 values of sWAT and iBAT volume

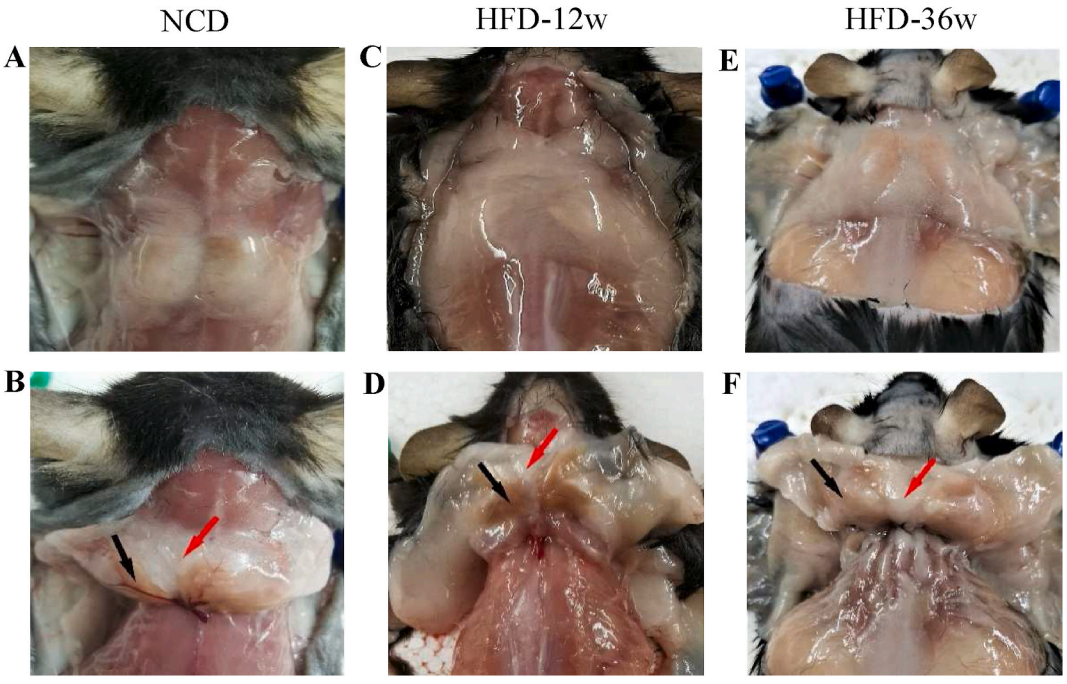

Fig. 1. Anatomical images of iBAT of mice after feeding on NCD for 12 weeks and HFD for 12 weeks and 36 weeks. The black arrow indicates iBAT, and the red arrow indicates sWAT. iBAT, interscapular brown adipose tissue; sWAT, subcutaneous white adipose tissue; NCD, normal chow diet; HFD, high-fat diet. (For interpretation of the references to colour in this figure legend, the reader is referred to the Web version of this article.)

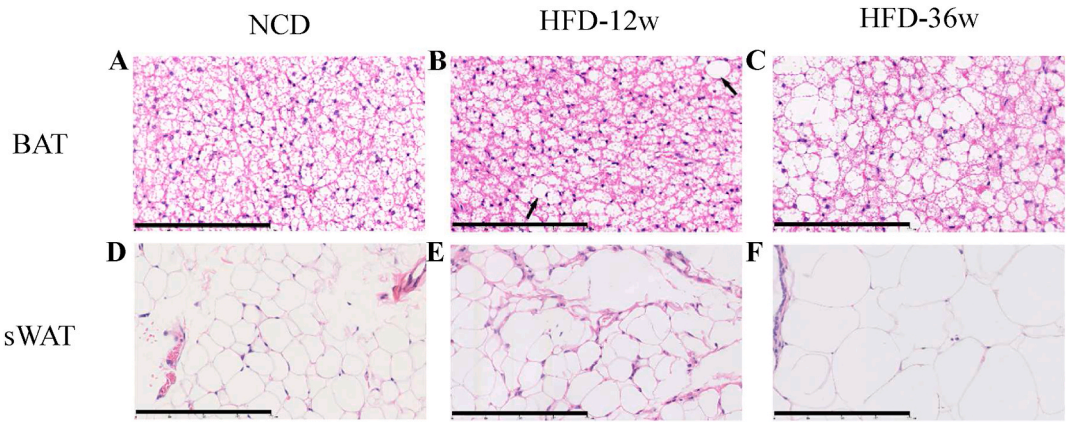

Fig. 2. HFD affects BAT and sWAT architecture. Histological results of representative Hematoxylin and eosin-stained BAT and sWAT images in three groups (scale bars = 200 μm). (A) BAT in the NCD group exhibited smaller multilocular adipocytes with a considerable volume of the cytoplasm. (B) Small numbers of large unilocular adipocyte accumulation were observed in the HFD-12w group (black arrow), indicating that BAT has been slightly whitened. (C) A large number of brown adipocytes in the HFD-36w group transformed from small multilocular to large unilocular adipocytes with a white-like appearance, accompanied by a complete structural disarrangement, indicating more severe whitening in BAT. (D) sWAT in the NCD group exhibited a single large unilocular lipid droplet with an intracellular eccentric nucleus. (E) Adipocytes within sWAT in the HFD-12w seems similar to the NCD group. (F) Adipocytes within sWAT in the HFD-36w group became larger. BAT, brown adipose tissue; sWAT, subcutaneous white adipose tissue; NCD, normal chow diet; HFD, high-fat diet. (For interpretation of the references to colour in this figure legend, the reader is referred to the Web version of this article.)

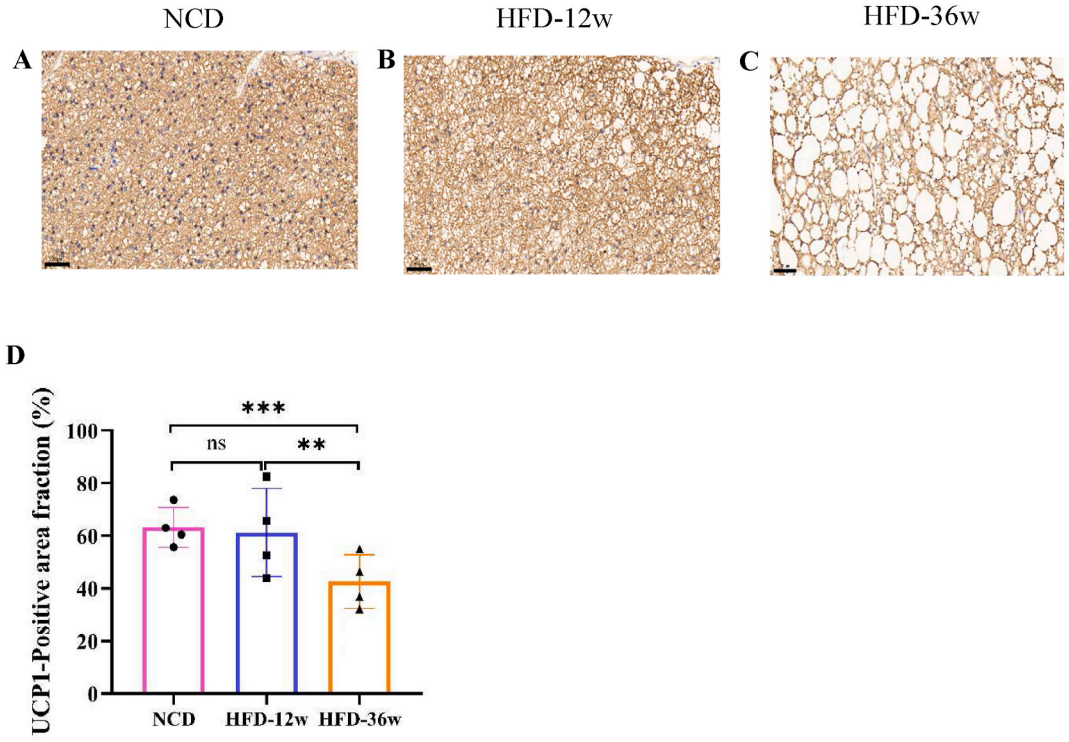

Fig. 3. HFD affects UCP1 expression in BAT. (A–C) Representative images of UCP1 immunohistochemistry in BATs (scale bars = 50 μm) showing positive immunoreactions in all groups (labeled in brown). (D) UCP1 quantification. Each column represents the mean ± SD; n = 4 for each group, n denotes biologically independent samples. Statistical significance was determined using one-way ANOVA with Bonferroni correction, where *P < 0.017 (alpha: 0.05/3), **P < 0.01, ***P < 0.001 indicates the degree of significance, and ns represents non-significant. BAT, brown adipose tissue; UCP1, uncoupling protein 1; NCD, normal chow diet; HFD, high-fat diet. (For interpretation of the references to colour in this figure legend, the reader is referred to the Web version of this article.)

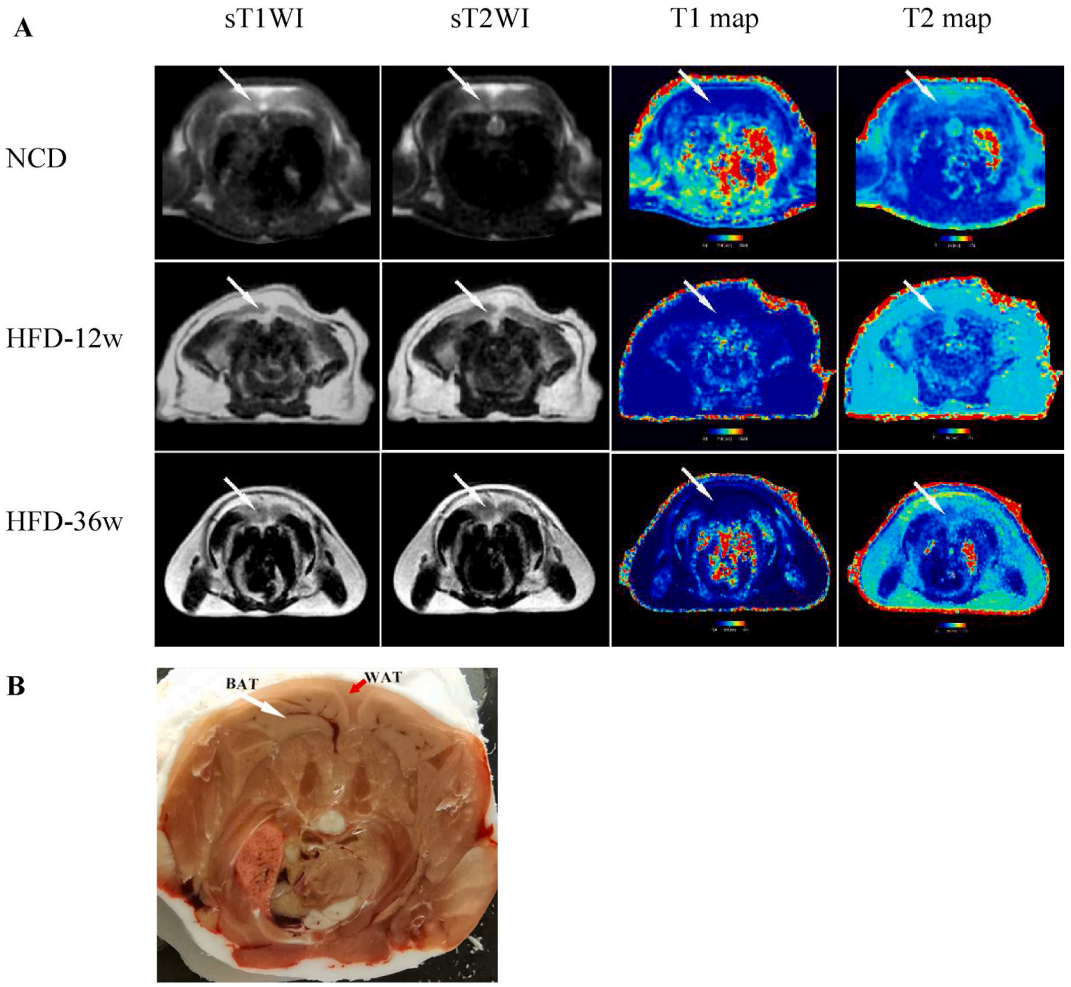

Fig. 4. Representative SyMRI images of iBAT in the three groups and representative photograph of axial cryosection. (A) The axial sT1WI, sT2WI, T1 map and T2 map of iBAT in the three groups. (B) The representative photograph of axial cryosection as anatomical reference. The white arrow indicates iBAT, and the red arrow indicates sWAT. iBAT, interscapular brown adipose tissue; sWAT, subcutaneous white adipose tissue; sT1WI, synthetic T1-weighted image; sT2WI, synthetic T2-weighted image; NCD, normal chow diet; HFD, high-fat diet. (For interpretation of the references to colour in this figure legend, the reader is referred to the Web version of this article.)

among the three groups ($P < 0.0001$, $P = 0.009$, respectively). Further analysis with the Bonferroni test revealed that the T2 values of sWAT and iBAT volume in the HFD-12w group (90.27 ± 5.45 ms, 0.073 ± 0.013 mL) was higher than that in NCD group (82.71 ± 8.28 ms, $P = 0.035$; 0.072 ± 0.01 mL, $P = 0.723$, respectively) but with no significant difference. In contrast, T2 values of sWAT and the iBAT volume in the HFD-36w group (97.86 ± 6.36 ms, 0.315 ± 0.105 mL) was significantly higher than that in the HFD-12w ($P = 0.001$, $P = 0.013$, respectively) and NCD groups ($P < 0.0001$, $P = 0.005$, respectively) (Fig. 5D and E).

3.3. Alterations serum lipid profiles and body weight during BAT whitening

One-way ANOVA revealed there were statistically significant difference among the three groups in the average serum levels of TG, TC, and HDL-C ($F = 36.63$, $P < 0.001$; $F = 11.053$, $P < 0.05$; $F = 15.442$, $P < 0.001$, respectively), and the Kruskal–Wallis test revealed a statistically significant difference among the three groups in the distribution of serum LDL-C level ($P = 0.008$). Further analysis with the Bonferroni test indicated that the serum levels of TG, TC, and LDL-C were significantly higher in the HFD-12w (2.51 ± 0.24 mmol/L, $P < 0.001$; 5.66 ± 0.39 mmol/L, $P = 0.002$; 3.39 ± 0.53 mmol/L, $P = 0.016$, respectively) and HFD-36w groups (2.73 ± 0.42 mmol/L, $P < 0.001$; 5.74 ± 0.40 mmol/L, $P = 0.001$; 4.00 ± 1.11 mmol/L, $P = 0.004$, respectively) than in the NCD group (1.22 ± 0.21 mmol/L, 4.44 ± 0.64 mmol/L, 1.26 ± 0.23 mmol/L, respectively), and the serum HDL-C level was significantly higher in the NCD group (2.85 ± 0.38 mmol/L) than in the HFD-12w (2.01 ± 0.61 mmol/L, $P = 0.011$) and HFD-36w groups (1.31 ± 0.25 mmol/L, $P < 0.001$), but no statistically significant differences were detected between the HFD-12w and HFD-36w group in serum levels of TG, TC, LDL-C and HDL-C ($P = 0.276$, $P = 0.806$, $P = 0.621$, $P = 0.027$, respectively) (Fig. 6A–D).

One-way ANOVA revealed a statistically significant difference in the average body weight of the mice among the three groups ($F =$

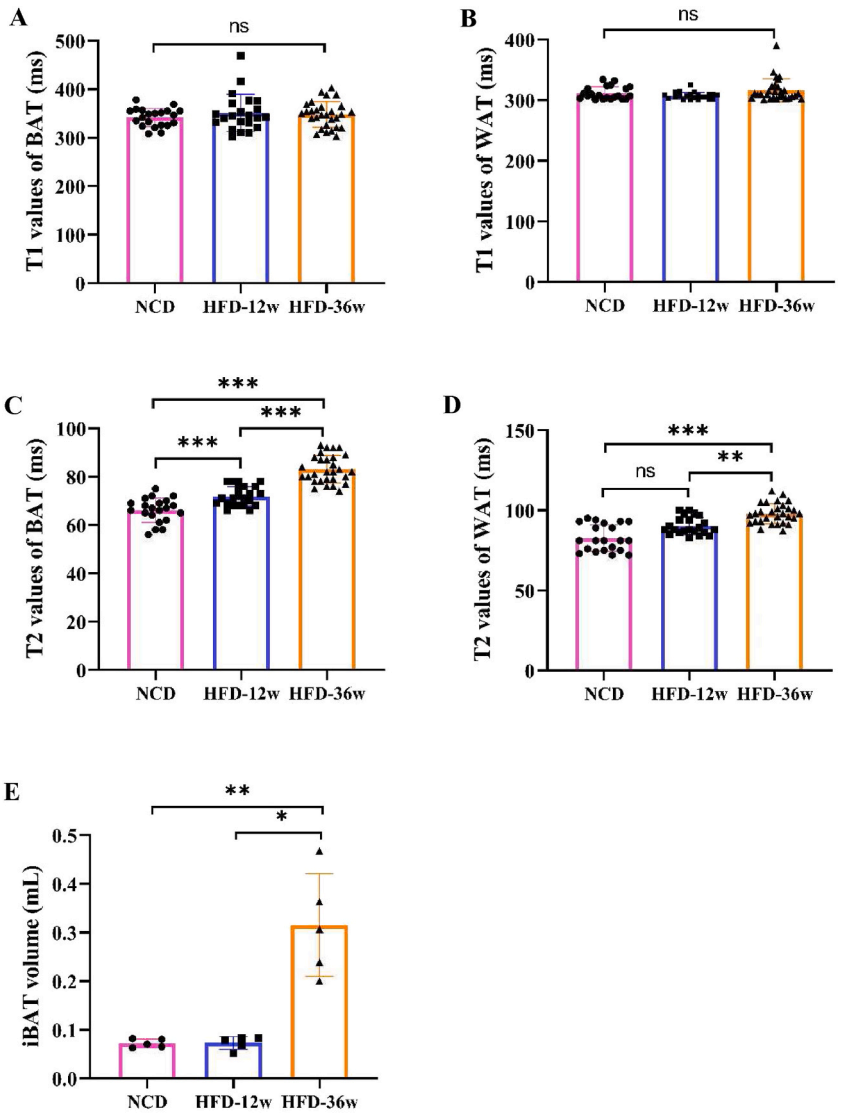

Fig. 5. T1 and T2 values of BAT and sWAT of mice and iBAT volume of the three groups measured by SyMRI. (A–D) T1 and T2 values of BAT and sWAT of the three groups. (NCD, n = 21, HFD-12w, n = 22, HFD-36w, n = 29, n denotes the number of slices of BAT measured on the sT2WI). (E) The iBAT volume of the three groups. (n = 5, n denotes biologically independent samples). Each column represents the mean ± SD. Statistical significance was determined using the Kruskal–Wallis test with Bonferroni correction for T1 values of BAT, T1 and T2 values of sWAT, and iBAT volume, and one-way ANOVA with Bonferroni correction for T2 values of BAT, where *P < 0.017 (alpha: 0.05/3), **P < 0.01, ***P < 0.001 indicates the degree of significance, and ns represents non-significant. iBAT, interscapular brown adipose tissue; sWAT, subcutaneous white adipose tissue; NCD, normal chow diet; HFD, high-fat diet; sT2WI, synthetic T2-weighted image. (For interpretation of the references to colour in this figure legend, the reader is referred to the Web version of this article.)

116.707, P < 0.001). Further analysis with the Bonferroni test indicated that the average body weight of mice in the HFD-12w group (33.32 ± 2.32 g) was significantly higher than that in the NCD group (27.36 ± 1.07 g, P = 0.01), whereas that in the HFD-36w group (55.89 ± 4.75 g) was significantly higher than that in the NCD and HFD-12w groups (both P < 0.001) (Fig. 6E).

3.4. Correlation between SyMRI quantitative values of BAT, serum lipid profiles, iBAT volume, and body weight

The T1 values of BAT showed no association with serum levels of TG, TC, LDL-C, and HDL-C (r = 0.218, P = 0.436; r = 0.324, P = 0.238; r = 0.380, P = 0.163; r = 0.059, P = 0.836, respectively) and body weight (r = 0.179, P = 0.524).

The correlation analysis results with T2 values are presented in Fig. 7. T2 values of BAT were moderately positively associated with serum levels of TG, TC, and LDL-C, and iBAT volume (r = 0.636, P = 0.011; r = 0.586, P = 0.022; r = 0.550, P = 0.034; r = 0.708, P = 0.003, respectively) (Fig. 7A–C, 7E), moderately negatively associated with serum HDL-C level (r = −0.738, P = 0.002) (Fig. 7D), and

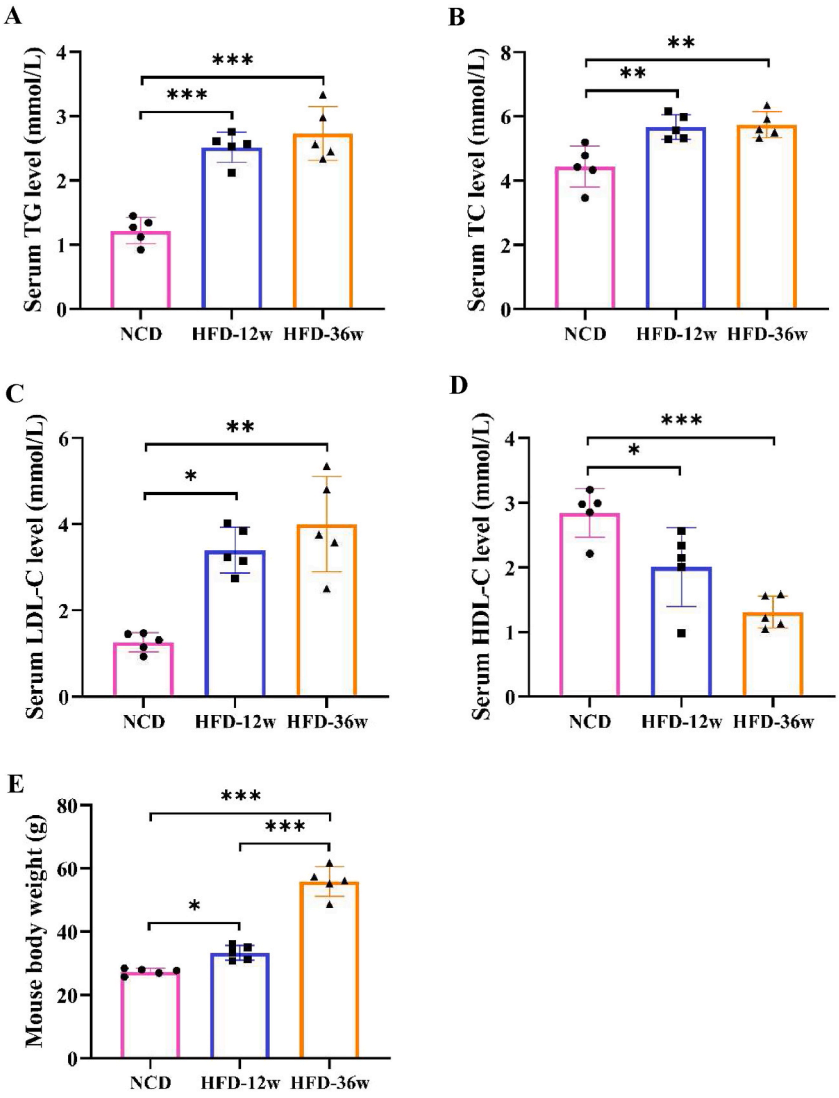

Fig. 6. Serum levels of TG, TC, LDL-C, and HDL-C and body weight of mice in the three groups. Serum levels comparisons of (A) TG, (B) TC, (C) LDL-C, and (D) HDL-C among the three groups. (E) Body weight comparison of mice among the three groups. Each column represents the mean ± SD, n = 5 for each group, n denotes biologically independent samples. Statistical significance was determined using one-way ANOVA with Bonferroni correction for serum levels of TG, TC, and HDL-C and body weight of mice, and the Kruskal–Wallis test with Bonferroni correction for serum level of LDL-C, where *P < 0.017 (alpha: 0.05/3), **P < 0.01, ***P < 0.001 indicates the degree of significance. TG, triglyceride; TC, total cholesterol; LDL-C, low-density lipoprotein cholesterol; HDL-C, high-density lipoprotein cholesterol; NCD, normal chow diet; HFD, high-fat diet.

strongly positively associated with body weight of mice (r = 0.833, P < 0.001) (Fig. 7F).

3.5. Correlation between iBAT volume, serum lipid profiles, body weight, and UCP1 quantitation

The correlation analysis results with iBAT volume are presented in Fig. 8. The iBAT volume measured by SyMRI was moderately positively associated with body weight (r = 0.706, P = 0.003) (Fig. 8A), moderately negatively associated with serum HDL-C level (r = −0.568, P = 0.027) (Fig. 8B), and highly negatively associated with the immunopositive area fraction of UCP1 (r = −0.846, P = 0.001) (Fig. 8C). However, no significant association with serum levels of TG, TC, and LDL-C (r = 0.315, P = 0.253; r = 0.415, P = 0.124; r = 0.454, P = 0.089, respectively) was observed.

4. Discussion

In the present study, SyMRI, histological, and statistical analyses indicated that a chronic HFD could induce BAT in mice to progressively whiten, accompanied by a decrease in UCP1 expression, body weight gain, and the corresponding changes in T2 values of

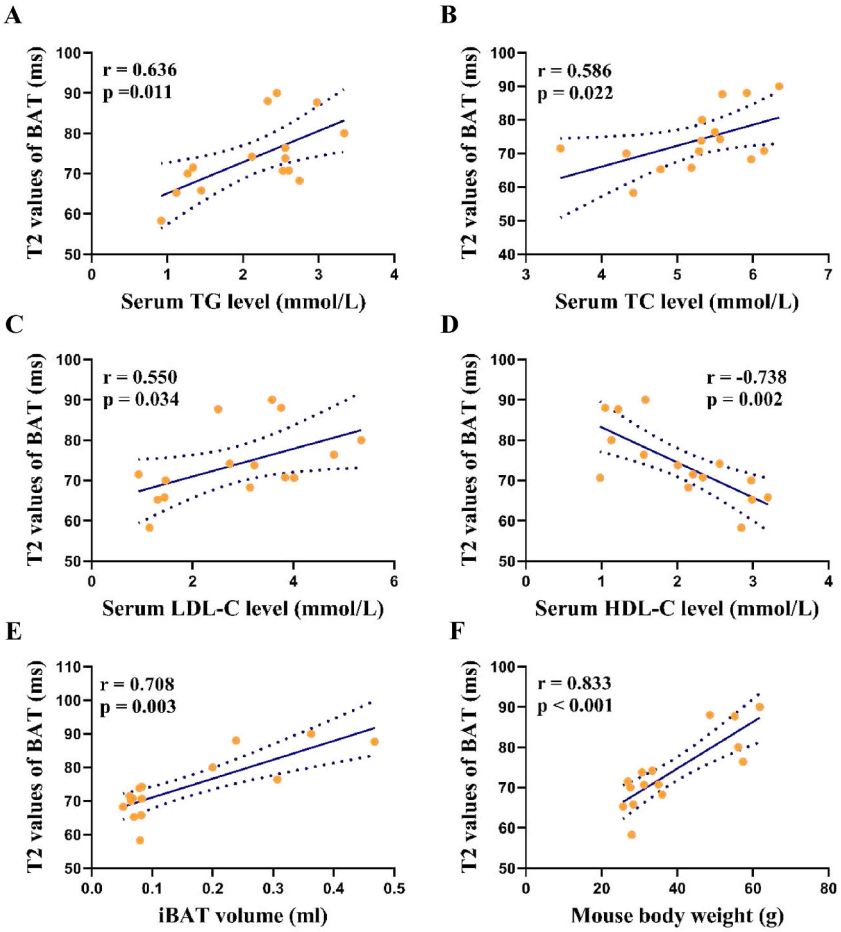

Fig. 7. Correlation between the T2 values of BAT with serum levels of TG, TC, LDL-C, and HDL-C, and mouse body weight. T2 values of BAT were positively correlated with serum levels of (A) TG, (B) TC, and (C) LDL-C, (E) iBAT volume, and (F) mouse body weight and inversely correlated with (D) serum level of HDL-C. iBAT, interscapular brown adipose tissue; TG, triglyceride; TC, total cholesterol; LDL-C, low-density lipoprotein cholesterol; HDL-C, high-density lipoprotein cholesterol. (For interpretation of the references to colour in this figure legend, the reader is referred to the Web version of this article.)

BAT and iBAT volume. Our results demonstrated that SyMRI is a quantitative technique that can noninvasively visualize the whitening process of BAT. We demonstrated the importance of assessing changes in BAT whitening using quantitative methods, especially to evaluate the therapeutic effects of drugs targeting these processes.

Adipose tissue is a highly plastic and dynamic tissue [24]. The plasticity of BAT and WAT determines whether an individual phenotype is obese or thin [25]. The metabolism, structure, and phenotype of adipose tissue can have significant changes under various physiological and pathological conditions [24,25]. WAT can acquire a brown-like phenotype by various stimuli, such as cold exposure and β-adrenergic receptor agonists, this progress is called browning [24–27]. BAT whitening induced by various interventions, such as HFD and chronic glucocorticoid exposure can lead to obesity and insulin resistance [1,4,9,28]. HFD-induced obesity affected the morphology of BAT, which was confirmed by anatomical observations, and histological staining in this study. BAT whitening caused reduced UCP1 expression, and impaired its main function, the non-shivering thermogenesis [9]. Of note, the HFD12-w showed unchanged UCP1 expression similar to the NCD group. However, the HFD-36w showed a significant decline in UCP1 expression, suggesting a time-dependent effect of the HFD on BAT function, this is similar to the study of Camilla Rangel-Azevedo [9].

SyMRI is an ideal method for measuring the degree of BAT whitening owing to its high spatial resolution, excellent soft tissue contrast, and noninvasive features. In this study, SyMRI analysis of mice fed an HFD from 12 to 36 weeks showed a progressive increase in T2 values of BAT, accompanied by an increase in large unilocular lipid droplets, suggesting a progressive BAT whitening, which was also observed in the histopathological analysis of BATs. In other words, the progress of BAT whitening was confirmed by T2 values and histological staining in the present study. Previous studies in normal lean mice have shown that the T2 values of BAT were lower than those of WAT, which is related to the fact that BAT contains rich vasculature and high iron content in the mitochondria [14,29]. We speculate that the gradual increase in T2 values with the progress of BAT whitening could be attributed to the following reasons. First, enlarged unilocular lipid droplet accumulation in BAT results in increased fat content and morphological changes. T2 values are influenced by fat fluidity, more saturated fatty acid lowers the fluidity, and low fluidity shortens the T2 values [30,31]. Subtle changes

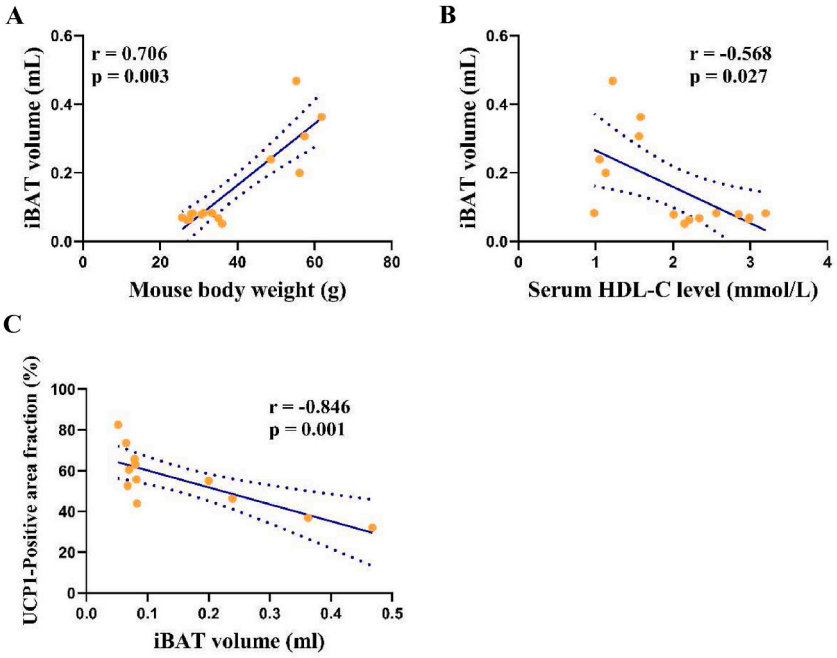

Fig. 8. Correlation between iBAT volume and mouse body weight, serum HDL-C level, and UCP1 quantitation. The iBAT volume was positively correlated with (A) mouse body weight and inversely correlated with (B) serum HDL-C level, and (C) the immunopositive area fraction of UCP1. iBAT, interscapular brown adipose tissue; HDL-C, high-density lipoprotein cholesterol; UCP1, uncoupling protein 1. (For interpretation of the references to colour in this figure legend, the reader is referred to the Web version of this article.)

of unsaturated fatty acid (UFA) content can affect fat fluidity(31). BAT has more saturated triglyceride and lower UFA content compared to WAT [32,33]. We speculate that UFA content changed between the BAT and the whitened BAT, resulting in increased T2 values of the whitened BAT. However, further studies are needed to verify this conjecture. Second, the progress of BAT whitening, corresponding to exhibits vascular rarefaction, blood flow reduction, the loss of mitochondria and reduced expression of UCP1, could lead to a functional change [4,34]. Previous study had shown that chronic high fat diet caused BAT whitening, and Vegfa expression was significantly down-regulated after mice were fed on HFD for 12, 16 and 20 weeks compared to that of mice on NCD, the interaction of enlarged lipid droplets and decreased vascularization aggravates BAT whitening [9], which would result in an increase in T2 values of BAT. Therefore, the morphological and functional changes in BAT during the whitening process could be quantitatively reflected by the T2 values of a quick SyMRI scan. In addition, T2 values of sWAT increased after mice fed an HFD from 12 to 36 weeks, and histologically, adipocytes within the sWAT initially appeared to be unilocular but became larger during the whitening process.

In the present study, the statistical analysis revealed that T2 values of BAT have a strong positive correlation with the body weight of mice and a moderate correlation with the serum lipid profiles, which indicated that SyMRI could display the process of BAT whitening in a noninvasive manner corresponding to the internal body alteration. The changes in the T2 values of BAT among the three groups were consistent with the changes in the body weight of mice, suggesting that the T2 values of BAT could reflect the change in body weight. As for the alteration of the serum liquid profiles, the T2 values of BAT of mice were moderately positively correlated with the serum levels of TG, TC, and LDL-C and moderately negatively correlated with the serum level of HDL-C. Overall, these analyses revealed that the real-time T2 values of mouse BAT could reflect the change in the serum lipid profile to a certain extent, which could be used as an indicator to evaluate the change in serum levels of TG, TC, LDL-C, and HDL-C.

In the present study, the T1 values of BAT were slightly different within the two HFD groups. However, they showed no significant difference among the three groups, indicating that BAT whitening had a limited effect on the T1 values of BAT. T1 values are usually related to fat content [15]. In the present study, the histopathology of BAT in the HFD-36w group showed a large number of enlarged lipid droplets in BAT cells, suggesting the increase of fat content. However, the T1 values of BAT did not significantly change as the fat content increased. This effect might be because the change in T1 values occurs later than that in T2 values during the whitening process of BAT.

In our study, the iBAT volume measured by SyMRI was positively correlated with the body weight of mice, which was consistent with the results of previous studies [14,29,35]. Moreover, there was no significant difference in the iBAT volume between the HFD-12w and NCD groups, suggesting that short-term HFD feeding which induced slight BAT whitening have little effect on the iBAT volume. However, slight BAT whitening could cause an increase in T2 values of BAT. Therefore, the T2 values of BAT in mice were more sensitive to changes of BAT whitening than the iBAT volume. Additionally, the iBAT volume of the HFD-36w group were significantly higher than that of the other groups, suggesting the iBAT volume increased because of a lot of larger unilocular lipid droplets full in BAT cells caused by long-term HFD feeding, therefore, the increase of iBAT volume reflected relatively severe whitening

of BAT. In this study, the iBAT volume is inversely correlated with the immunopositive area fraction of UCP1. The immunopositive area fraction of UCP1 reflect BAT activity to some extent. We speculate that iBAT volume is inversely correlated with BAT activity at room temperature (20–24 °C), because HFD increases iBAT volume [36], in obese mice, BAT is swollen with fat, and UCP1 content is considerably reduced in the BAT(34). BAT activity is related to age, environmental temperature and body fat content. BAT activity and volume had been increased after acute cold exposure [37], so it is unclear whether iBAT volume correlates to BAT activity after cold exposure. Therefore, the increase in the iBAT volume is another indicator of BAT whitening at room temperature.

The present study has certain limitations. The HFD-36w group lacked age-matched normal controls because our study focused on the quantitative evaluation of BAT whitening processes using SyMRI. In addition, the BAT wet weight was not measured in this study because it was challenging to identify and remove WAT around BAT in HFD-fed mice with the naked eye.

5. Conclusion

In conclusion, we confirmed that SyMRI could noninvasively evaluate the process of BAT whitening with derived T2 values and iBAT volume. T2 values played an important role in visualizing the whitening process of BAT and were significantly correlated with the serum lipid profiles and body weight. The results from SyMRI suggest its potential in objectively and noninvasively quantitatively assessing the BAT whitening process and alteration in serum lipid profiles for the treatment of obesity and metabolic diseases in the future.

Ethics approval and consent to participate

This study was approved by the Institutional Animal Care and Use Committee of Sun Yat-sen University (Approval number: [2021] 862). All animal experiments were performed in compliance with the institutional guidelines for the care and use of animals. All experiments complied with the ARRIVE Guidelines.

Funding

This work was funded by the National Natural Science Foundation of China (82271958, 82001882), the Natural Science Foundation of Guangdong Province (2021A1515011442), and the Scientific Research Project of Traditional Chinese Medicine Bureau of Guangdong Province (20211173).

Data availability statement

Data will be made available on request.

CRediT authorship contribution statement

Mengjuan Huo: Writing – review & editing, Writing – original draft, Methodology, Data curation, Conceptualization. **Junzhao Ye:** Writing – original draft, Methodology, Data curation, Conceptualization. **Yinhong Zhang:** Writing – original draft, Methodology, Data curation, Conceptualization. **Meng Wang:** Writing – original draft, Methodology, Data curation. **Jialu Zhang:** Writing – original draft, Software, Methodology. **Shi-Ting Feng:** Writing – original draft, Methodology, Funding acquisition, Conceptualization. **Huasong Cai:** Writing – review & editing, Writing – original draft, Methodology, Data curation, Conceptualization. **Bihui Zhong:** Writing – review & editing, Writing – original draft, Supervision, Resources, Project administration, Conceptualization. **Zhi Dong:** Writing – review & editing, Writing – original draft, Supervision, Project administration, Methodology, Funding acquisition, Conceptualization.

Declaration of competing interest

The authors declare that they have no known competing financial interests or personal relationships that could have appeared to influence the work reported in this paper.

Acknowledgments

The authors thank Dr. Long Qian for help in solving the MR technical problems.

References

[1] P. Kotzbeck, A. Giordano, E. Mondini, I. Murano, I. Severi, W. Venema, M.P. Cecchini, E.E. Kershaw, G. Barbatelli, G. Haemmerle, R. Zechner, S. Cinti, Brown adipose tissue whitening leads to brown adipocyte death and adipose tissue inflammation, J. Lipid Res. 59 (5) (2018) 784–794, https://doi.org/10.1194/jlr.M079665.

[2] L. Deng, Z. Ou, D. Huang, C. Li, Z. Lu, W. Liu, F. Wu, C. Nong, J. Gao, Y. Peng, Diverse effects of different Akkermansia muciniphila genotypes on Brown adipose tissue inflammation and whitening in a high-fat-diet murine model, Microb. Pathog. 147 (2020) 104353, https://doi.org/10.1016/j.micpath.2020.104353.

[3] J. Deng, Y. Guo, F. Yuan, S. Chen, H. Yin, X. Jiang, F. Jiao, F. Wang, H. Ji, G. Hu, H. Ying, Y. Chen, Q. Zhai, F. Xiao, F. Guo, Autophagy inhibition prevents glucocorticoid-increased adiposity via suppressing BAT whitening, Autophagy 16 (3) (2020) 451–465, https://doi.org/10.1080/15548627.2019.1628537.

[4] I. Shimizu, T. Aprahamian, R. Kikuchi, A. Shimizu, K.N. Papanicolaou, S. MacLauchlan, S. Maruyama, K. Walsh, Vascular rarefaction mediates whitening of brown fat in obesity, J. Clin. Invest. 124 (5) (2014) 2099–2112, https://doi.org/10.1172/JCI71643.

[5] F. Lopez-Vicchi, C. De Winne, A.M. Ornstein, E. Sorianello, J. Toneatto, D. Becu-Villalobos, Severe hyperprolactinemia promotes Brown adipose tissue whitening and aggravates high fat diet induced metabolic imbalance, Front. Endocrinol. 13 (2022) 883092, https://doi.org/10.3389/fendo.2022.883092.

[6] K. Takaishi, T. Oshima, H. Eto, M. Nishihira, S.T. Nguyen, R. Ochi, N. Fujita, S. Urakawa, Impact of exercise and detraining during childhood on Brown adipose tissue whitening in obesity, Metabolites 11 (10) (2021) 677, https://doi.org/10.3390/metabo11100677.

[7] P. Gao, Y. Jiang, H. Wu, F. Sun, Y. Li, H. He, B. Wang, Z. Lu, Y. Hu, X. Wei, Y. Cui, C. He, L. Wang, H. Zheng, G. Yang, D. Liu, Z. Yan, Z. Zhu, Inhibition of mitochondrial calcium overload by SIRT3 prevents obesity- or age-related whitening of Brown adipose tissue, Diabetes 69 (2) (2020) 165–180, https://doi.org/10.2337/db19-0526.

[8] C.S. Miranda, F. Silva-Veiga, F.F. Martins, T.L. Rachid, C.A. Mandarim-De-Lacerda, V. Souza-Mello, PPAR-α activation counters brown adipose tissue whitening: a comparative study between high-fat- and high-fructose-fed mice, Nutrition 78 (2020) 110791, https://doi.org/10.1016/j.nut.2020.110791.

[9] C. Rangel-Azevedo, D.A. Santana-Oliveira, C.S. Miranda, F.F. Martins, C.A. Mandarim-de-Lacerda, V. Souza-Mello, Progressive brown adipocyte dysfunction: whitening and impaired nonshivering thermogenesis as long-term obesity complications, J. Nutr. Biochem. 105 (2022) 109002, https://doi.org/10.1016/j.jnutbio.2022.109002.

[10] B. Cannon, J.M.A. de Jong, A.W. Fischer, J. Nedergaard, N. Petrovic, Human brown adipose tissue: classical brown rather than brite/beige? Exp. Physiol. 105 (8) (2020) 1191–1200, https://doi.org/10.1113/EP087875.

[11] J.M.A. de Jong, W. Sun, N.D. Pires, A. Frontini, M. Balaz, N.Z. Jespersen, A. Feizi, K. Petrovic, A.W. Fischer, M.H. Bokhari, T. Niemi, P. Nuutila, S. Cinti, S. Nielsen, C. Scheele, K. Virtanen, B. Cannon, J. Nedergaard, C. Wolfrum, N. Petrovic, Human brown adipose tissue is phenocopied by classical brown adipose tissue in physiologically humanized mice, Nat. Metab. 1 (8) (2019) 830–843, https://doi.org/10.1038/s42255-019-0101-4.

[12] N.M. Kumar, B. Fritz, S.E. Stern, J.B.M. Warntjes, Y.M. Lisa Chuah, J. Fritz, Synthetic MRI of the knee: phantom validation and comparison with conventional MRI, Radiology 289 (2) (2018) 465–477, https://doi.org/10.1148/radiol.2018173007.

[13] Y. Arita, T. Takahara, S. Yoshida, T.C. Kwee, S. Yajima, C. Ishii, R. Ishii, S. Okuda, M. Jinzaki, Y. Fujii, Quantitative assessment of bone metastasis in prostate cancer using synthetic magnetic resonance imaging, Invest. Radiol. 54 (10) (2019) 638–644, https://doi.org/10.1097/RLI.0000000000000579.

[14] M. Huo, J. Ye, Z. Dong, H. Cai, M. Wang, G. Yin, L. Qian, Z.P. Li, B. Zhong, S.T. Feng, Quantification of brown adipose tissue in vivo using synthetic magnetic resonance imaging: an experimental study with mice model, Quant. Imag. Med. Surg. 12 (1) (2022) 526–538, https://doi.org/10.21037/qims-20-1344.

[15] N. Garnov, N. Linder, A. Schaudinn, M. Blüher, T. Karlas, T. Schütz, A. Dietrich, T. Kahn, H. Busse, Comparison of T1 relaxation times in adipose tissue of severely obese patients and healthy lean subjects measured by 1.5 T MRI, NMR Biomed. 27 (9) (2014) 1123–1128, https://doi.org/10.1002/nbm.3166.

[16] F. Binayi, M. Moslemi, F. Khodagholi, M. Hedayati, H. Zardooz, Long-term high-fat diet disrupts lipid metabolism and causes inflammation in adult male rats: possible intervention of endoplasmic reticulum stress, Arch. Physiol. Biochem. 129 (1) (2023) 204–212, https://doi.org/10.1080/13813455.2020.1808997.

[17] I. Shimizu, K. Walsh, The whitening of Brown fat and its implications for weight management in obesity, Curr. Obes. Rep. 4 (2) (2015) 224–229, https://doi.org/10.1007/s13679-015-0157-8.

[18] K.M. Kang, S.H. Choi, M. Hwang, T.J. Yun, J.H. Kim, C.H. Sohn, T1 shortening in the globus pallidus after multiple administrations of gadobutrol: assessment with a multidynamic multiecho sequence, Radiology 287 (1) (2018) 258–266, https://doi.org/10.1148/radiol.2017162852.

[19] S.M. Lee, Y.H. Choi, S.K. You, W.K. Lee, W.H. Kim, H.J. Kim, S.Y. Lee, H. Cheon, Age-related changes in tissue value properties in children: simultaneous quantification of relaxation times and proton density using synthetic magnetic resonance imaging, Invest. Radiol. 53 (4) (2018) 236–245, https://doi.org/10.1097/RLI.0000000000000435.

[20] Y. Cui, S. Han, M. Liu, P.Y. Wu, W. Zhang, J. Zhang, C. Li, M. Chen, Diagnosis and grading of prostate cancer by relaxation maps from synthetic MRI, J. Magn. Reson. Imag. 52 (2) (2020) 552–564, https://doi.org/10.1002/jmri.27075.

[21] Y.L. Wong, L. LeBon, A.M. Basso, K.L. Kohlhaas, A.L. Nikkel, H.M. Robb, D.L. Donnelly-Roberts, J. Prakash, A.M. Swensen, N.D. Rubinstein, S. Krishnan, F. E. McAllister, N.V. Haste, J.J. O'Brien, M. Roy, A. Ireland, J.M. Frost, L. Shi, S. Riedmaier, K. Martin, M.J. Dart, C. Sidrauski, eIF2B activator prevents neurological defects caused by a chronic integrated stress response, Elife 8 (2019) e42940, https://doi.org/10.7554/eLife.42940.

[22] H. Okasha, A.M. Abu-Seida, A.A. Hashem, S.H. El Ashry, M.M. Nagy, Inflammatory response and immunohistochemical characterization of experimental calcium silicate-based perforation repair material, Int. J. Exp. Pathol. 103 (4) (2022) 156–163. https://doi.org/10.1111/iep.12439.

[23] C.S. Jung, M. Heine, B. Freund, R. Reimer, E.J. Koziolek, M.G. Kaul, F. Kording, U. Schumacher, H. Weller, P. Nielsen, G. Adam, J. Heeren, H. Ittrich, Quantitative activity measurements of Brown adipose tissue at 7 T magnetic resonance imaging after application of triglyceride-rich lipoprotein 59Fe-superparamagnetic iron oxide nanoparticle: intravenous versus intraperitoneal approach, Invest. Radiol. 51 (3) (2016) 194–202, https://doi.org/10.1097/RLI.0000000000000235.

[24] L. Li, Q. Wan, Q. Long, T. Nie, S. Zhao, L. Mao, C. Cheng, C. Zou, K. Loomes, A. Xu, L. Lai, X. Liu, Z. Duan, X. Hui, D. Wu, Comparative transcriptomic analysis of rabbit interscapular brown adipose tissue whitening under physiological conditions, Adipocyte 11 (1) (2022) 529–549. https://doi.org/10.1080/21623945.2022.2111053.

[25] S. Lim, J. Honek, Y. Xue, T. Seki, Z. Cao, P. Andersson, X. Yang, K. Hosaka, Y. Cao, Cold-induced activation of brown adipose tissue and adipose angiogenesis in mice, Nat. Protoc. 7 (3) (2012) 606–615. https://doi.org/10.1038/nprot.2012.013.

[26] S. Collins, K.W. Daniel, A.E. Petro, R.S. Surwit, Strain-specific response to beta 3-adrenergic receptor agonist treatment of diet-induced obesity in mice, Endocrinology 138 (1) (1997) 405–413. https://doi.org/10.1210/endo.138.1.4829.

[27] N. Martínez-Sánchez, There and back again: leptin actions in white adipose tissue, Int. J. Mol. Sci. 21 (17) (2020) 6039. https://doi.org/10.3390/ijms21176039.

[28] J.S. Bel, T.C. Tai, N. Khaper, S.J. Lees, Chronic glucocorticoid exposure causes brown adipose tissue whitening, alters whole-body glucose metabolism and increases tissue uncoupling protein-1, Phys. Rep. 10 (9) (2022) e15292, https://doi.org/10.14814/phy2.15292.

[29] Y.I. Chen, A.M. Cypess, C.A. Sass, A.L. Brownell, K.T. Jokivarsi, C.R. Kahn, K.K. Kwong, Anatomical and functional assessment of brown adipose tissue by magnetic resonance imaging, Obesity 20 (7) (2012) 1519–1526. https://doi.org/10.1038/oby.2012.22.

[30] R. Ouwerkerk, A. Hamimi, J. Matta, K.Z. Abd-Elmoniem, J.F. Eary, Z. Abdul Sater, K.Y. Chen, A.M. Cypess, A.M. Gharib, Proton MR spectroscopy measurements of white and Brown adipose tissue in healthy humans: relaxation parameters and unsaturated fatty acids, Radiology 299 (2) (2021) 396–406. https://doi.org/10.1148/radiol.2021202676.

[31] M.D. Robinson, D.P. Cistola, Nanofluidity of fatty acid hydrocarbon chains as monitored by benchtop time-domain nuclear magnetic resonance, Biochemistry 53 (48) (2014) 7515–7522. https://doi.org/10.1021/bi5011859.

[32] G. Hamilton, D.L. Smith, M. Bydder, K.S. Nayak, H.H. Hu, MR properties of brown and white adipose tissues, J. Magn. Reson. Imaging. 34 (2) (2011) 468–473. https://doi.org/10.1002/jmri.22623.

[33] B. Cannon, J. Nedergaard, Brown adipose tissue: function and physiological significance, Physiol. Rev. 84 (1) (2004) 277–359. https://doi.org/10.1152/physrev.00015.2003.

[34] R.T. Branca, T. He, L. Zhang, C.S. Floyd, M. Freeman, C. White, A. Burant, Detection of brown adipose tissue and thermogenic activity in mice by hyperpolarized xenon MRI, Proc. Natl. Acad. Sci. U.S.A. 111 (50) (2014) 18001–18006. https://doi.org/10.1073/pnas.1403697111.

[35] H.H. Hu, D.L. Smith Jr., K.S. Nayak, M.I. Goran, T.R. Nagy, Identification of brown adipose tissue in mice with fat-water IDEAL-MRI, J. Magn. Reson. Imaging. 31 (5) (2010) 1195–1202. https://doi.org/10.1002/jmri.22162.

[36] Z.J. D'Alonzo, J.C.L. Mamo, L.T. Graneri, R. Takechi, V. Lam, The effects of chronic consumption of lipid-rich and delipidated bovine dairy milk on Brown adipose tissue volume in wild-type mice, Nutrients 13 (12) (2021) 4266. https://doi.org/10.3390/nu13124266.

[37] C. Huo, Z. Song, J. Yin, Y. Zhu, X. Miao, H. Qian, J. Wang, L. Ye, L. Zhou, Effect of acute cold exposure on energy metabolism and activity of Brown adipose tissue in humans: a systematic review and meta-analysis, Front. Physiol. 13 (2022) 917084. https://doi.org/10.3389/fphys.2022.917084.